



Published in final edited form as:

Neuroimage. 2021 July 15; 235: 117974. doi:10.1016/j.neuroimage.2021.117974.

Maturational trajectories of pericortical contrast in typical brain development

Stefan Drakulich^{a,1}, Anne-Charlotte Thiffault^{a,1}, Emily Olafson^b, Olivier Parent^b, Aurelie Labbe^c, Matthew D. Albaugh^d, Budhachandra Khundrakpam^a, Simon Ducharme^a, Alan Evans^a, Mallar M. Chakravarty^{b,*}, Sherif Karama^{a,b,**}

^aMontreal Neurological Institute, McGill University, 3801 Rue University, Montréal, QC H3A 2B4, Canada

^bDouglas Institute, McGill University, 6875 Boulevard LaSalle, Verdun, QC H4H 1R3, Canada

^cHEC Montréal, 3000, chemin de la Côte-Sainte-Catherine, Montreal, QC H3T 2A7, Canada

^dDepartment of Psychiatry, Larnier College of Medicine, University of Vermont, United States

Abstract

In the last few years, a significant amount of work has aimed to characterize maturational trajectories of cortical development. The role of pericortical microstructure putatively characterized as the gray-white matter contrast (GWC) at the pericortical gray-white matter boundary and its relationship to more traditional morphological measures of cortical morphometry has emerged as a means to examine finer grained neuroanatomical underpinnings of cortical changes. In this work, we characterize the GWC developmental trajectories in a representative sample ($n = 394$) of children and adolescents (~4 to ~22 years of age), with repeated scans (1–3

This is an open access article under the CC BY-NC-ND license (<http://creativecommons.org/licenses/by-nc-nd/4.0/>)

*Corresponding author. mallar.chakravarty@douglas.mcgill.ca (M.M. Chakravarty). **Corresponding author at: Montreal Neurological Institute, McGill University, 3801 Rue University, Montréal, QC H3A 2B4, Canada, sherif.karama@mcgill.ca (S. Karama).

¹Primary contributors and contributed equally.

Credit authorship contribution statement

Stefan Drakulich: Methodology, Software, Formal analysis, Investigation, Writing – original draft, Writing – review & editing, Visualization. **Anne-Charlotte Thiffault:** Methodology, Software, Formal analysis, Investigation, Writing – original draft, Writing – review & editing. **Emily Olafson:** Methodology, Software, Visualization, Validation. **Olivier Parent:** Methodology, Software, Investigation. **Aurelie Labbe:** Methodology, Software, Validation. **Matthew D. Albaugh:** Methodology. **Budhachandra Khundrakpam:** Conceptualization, Methodology, Validation. **Simon Ducharme:** Conceptualization, Methodology, Validation. **Alan Evans:** Funding acquisition, Supervision. **Mallar M. Chakravarty:** Conceptualization, Methodology, Investigation, Writing – review & editing, Supervision. **Sherif Karama:** Conceptualization, Methodology, Investigation, Funding acquisition, Writing – original draft, Writing – review & editing, Supervision.

Data and Code Availability Statement

The NIHPD dataset used in this study can be found online (https://nda.nih.gov/edit_collection.html?id=1151). The CIVET 2.1.1 pipeline developed at the Montreal Neurological Institute was used to process T1-weighted images (<http://www.bic.mni.mcgill.ca/Services/Software/CIVET-2-1-0-References>). The SurfStat cortical surface analysis toolbox for Matlab is publicly available and can be freely downloaded online (<https://www.math.mcgill.ca/keith/surfstat/>). R Project version 3.6.2 was used, and can be freely obtained via CRAN, the “Comprehensive R Archive Network” (<https://cran.r-project.org/index.html>). Matlab version R2017b was used, and can be acquired with a license (<https://www.mathworks.com/products/matlab.html>). R package *nlme* version 3.1 was used for mixed-effects modeling (<https://cran.r-project.org/web/packages/nlme/nlme.pdf>).

Declaration of Competing Interest

None.

Supplementary materials

Supplementary material associated with this article can be found, in the online version, at doi:10.1016/j.neuroimage.2021.117974.

scans per subject, total scans $n = 819$). We tested whether linear, quadratic, or cubic trajectories of contrast development best described changes in GWC. A best-fit model was identified vertex-wise across the whole cortex via the Akaike Information Criterion (AIC). GWC across nearly the whole brain was found to significantly change with age. Cubic trajectories were likeliest for 63% of vertices, quadratic trajectories were likeliest for 20% of vertices, and linear trajectories were likeliest for 16% of vertices. A main effect of sex was observed in some regions, where males had a higher GWC than females. However, no sex by age interactions were found on GWC. In summary, our results suggest a progressive decrease in GWC at the pericortical boundary throughout childhood and adolescence. This work contributes to efforts seeking to characterize typical, healthy brain development and, by extension, can help elucidate aberrant developmental trajectories.

Keywords

Brain development; Gray-white contrast; Cortical contrast; Childhood; Adolescence; Structural MRI

1. Introduction

The human brain is a remarkably complex organ, with a dynamic development profile. By the fourth week of gestation, the brain's major cortical structures are formed (Muñoz-Moreno et al., 2016), though it continues to develop and organize new neuroanatomical pathways well into adulthood (Giedd and Rapoport, 2010; Lebel and Beaulieu, 2011; Shaw et al., 2008). Cortical maturation and the refinement of neuronal pathways have been shown to have direct links to children's behavior and cognitive performance and potentially contribute to identify maladaptive trajectories of development and associated neuropsychiatric disorders (Ducharme et al., 2014; Ducharme et al., 2012; Giedd et al., 2009; Giedd and Rapoport, 2010; Kharitonova et al., 2013; Lenroot et al., 2007; Shaw et al., 2011; Shaw et al., 2006, 2006; Thormodsen et al., 2013). Improving our knowledge of the neural development of healthy children and adolescents may hence allow us to identify atypical trajectories as well as critical developmental periods when a child's brain is most vulnerable to environmental influences.

Over the last three decades, neuroimaging has become an indispensable tool in brain research, allowing for in-vivo, non-invasive characterization of neurological structures at a submillimeter level of resolution (Ameis et al., 2014; Dosenbach et al., 2010; Giedd et al., 1999; Gogtay et al., 2004; Khundrakpam et al., 2016; Raznahan et al., 2011; Shaw et al., 2006, 2006; Thompson et al., 2000). Significant efforts have been made to accurately describe the developmental trajectory of several morphological features of the cortex as measured with magnetic resonance imaging (MRI). Cortical volume was one of the first cortical metrics to be longitudinally characterized and was reported, in earlier studies, to increase until late childhood and then to decrease afterwards (Giedd et al., 1999; Gogtay et al., 2004; Lenroot et al., 2007). Later studies have reported that cortical volume reached its peak in early childhood and decreased in later childhood and throughout adolescence (Lebel and Beaulieu, 2011; Mills et al., 2016; Mills et al., 2014; Tamnes et al., 2017, 2013).

In order to more precisely characterize cortical development, cortical volume measures can be effectively fractionated into cortical thickness and surface area components, which have been shown to be more susceptible to environment and genetics, respectively (Ducharme et al., 2015; Fischl et al., 1999; Ghosh et al., 2010; Patel et al., 2020; Postelnicu et al., 2009; Raznahan et al., 2011; Thompson et al., 2017). There have been inconsistencies between studies regarding the trajectory of cortical thickness development from mid-childhood to late adolescence (Tamnes et al., 2017). Some early work (Raznahan et al., 2011; Shaw et al., 2007) reported increasing thickness until late childhood followed by a decline afterwards while the majority of studies reported a general decrease with age during mid-childhood and adolescence (Alexander-Bloch et al., 2014; Ducharme et al., 2016; Fjell et al., 2015; Mills et al., 2014; Sowell et al., 2004; Tamnes et al., 2017; Zhou et al., 2015; Zielinski et al., 2014). As for surface area, the majority of studies report a tendency for an increase during childhood followed by a decrease during adolescence (Ducharme et al., 2015; Mills et al., 2014; Raznahan et al., 2011; Tamnes et al., 2017).

Recently, methods to measure T1-weighted (T1w) pericortical gray-to-white matter intensity ratio (referred to as “gray-white contrast”/GWC in this work), have been developed; GWC can be calculated as the ratio of the T1w signal intensity at a certain distance on either side of the gray-white cortical boundary. Some have used the gray to white ratio as their measure of contrast (Salat et al., 2009), with larger values representing less sharp pericortical boundaries, whereas others have instead used white to gray ratio as their measure of contrast, with larger values representing sharper pericortical boundaries (Lewis et al., 2018). In the current work, we adopt the white to gray ratio approach, with larger values representing sharper boundaries.

GWC is considered to be influenced by the development of pericortical microstructure including myelin invading the lower layers of the cortex during development (Dale et al., 1999; Grydeland et al., 2013; Norbom et al., 2019; Patel et al., 2020; Rowley et al., 2015; Vidal-Piñeiro et al., 2016). As such, GWC is thought to provide insight into subtle variations of neuronal tissue that are not otherwise captured by cortical thickness, area, or volume metrics alone. There are nonetheless likely certain relationships between GWC and these other MRI-based metrics. Indeed, the placement of the gray-white surface boundary is based on GWC and may hence influence estimates of cortical thickness, area, and volume. In fact, the invasion of myelin in the lower layers of the cortex may be responsible for part of the apparent reductions in MRI-based estimates of cortical thickness previously attributed exclusively to gray-matter processes. This sentiment is also put forth by Sowell et al. (2004), wherein they note that the invasion of the cortex by myelin may yield lower estimates of MRI-based cortical thickness.

Other studies that have worked on discerning the contributions of biological processes which drive maturational changes in the cortex have considered microstructural pericortical measures (such as GWC) as distinct and informative measures (Croteau-Chonka et al., 2016; Deoni et al., 2015; Norbom et al., 2019, 2020). For example, Croteau-Chonka et al. (2016) found that maturation of cortical thickness in early childhood in some regions of the cortex was unaffected by white-matter maturation, concluding that brain imaging studies of cortical and white matter maturation can reflect distinct, but complimentary, neurodevelopmental

processes. Importantly, GWC has previously been established as a metric linked to cognitive performance (Lewis et al., 2018), aging of the brain (Magnaldi et al., 1993; Raz et al., 2005), and developmental neuropsychopathology (Bezgin et al., 2018). Still, there is a relative paucity of studies in this domain, especially those seeking to disentangle the relative contributions of biological processes on either side of the pericortical gray-white boundary. The current study follows directly from previous efforts examining longitudinal pericortical maturation by providing a detailed characterization of the developmental trajectories of GWC in healthy children and adolescents (Brain Development Cooperative, 2012). This is the first study that uses repeated scans within a longitudinal design to examine GWC changes across the important maturational changes that occur in typically developing individuals between childhood and early adulthood.

2. Materials & Methods

2.1. Participants

Data were obtained from the longitudinal NIH Study of Normal Brain Development (Evans and Brain Development Cooperative, 2006). Study participants were recruited across six Pediatric Study Centers across the United States and ranged in age from 4.5 to 18.3 years ($N = 431$ participants; 207 M/224 F) at the first visit. They were selected using a population-based sampling plan aiming to recruit a sample representative of the US population, based on data from the 2000 US census (Brain Development Cooperative, 2012). More specifically, the sampling plan allowed to build a sample representative of the general US population (2000 census) by referencing geocoded census data. More specifically, recruitment was monitored continuously to maintain a demographically representative sample based on age, gender, ethnicity, and socioeconomic status variables (Evans and Brain Development Cooperative, 2006). Subjects were interviewed following the Diagnostic Interview for Children and Adolescents. Those found to have a major Axis I diagnosis according to DSM-IV classification, were excluded. Further, children with a Child Behavior Checklist syndrome T-score equal to or greater than 70, abnormal findings on neurological examination, or exposure during gestation to substances that may alter brain development, were also excluded. The full list of selection criteria can be accessed in Evans and Brain Development Cooperative (2006). Subjects underwent repeated magnetic resonance brain imaging (MRI) every 2 years, with a maximum of three scans over a 4-year period.

2.2. MRI protocol

Whole-brain 3D T1-weighted spoiled gradient recalled echo sequences were acquired on 1.5T MRI scanners across sites with a 1 mm isotropic resolution except for GE scanners which had an in-plane 1 mm isotropic but for which a 1.5 mm slice thickness was allowed due to their limit of 124 slices (Evans and Brain Development Cooperative, 2006). Inter-site reliability of anatomical measurements was assessed throughout the study by scanning phantoms of the American College of Radiology, as well as live volunteers regularly and at each site (Evans and Brain Development Cooperative, 2006; Kabani et al., 2001; Lerch and Evans, 2005). Scans were reviewed immediately after acquisition and repeated if there were either significant motion artifacts or field distortions. As described in Evans and Brain Development Cooperative (2006), only scans that passed raw MRI quality control were

included in the final release of the NIHPD dataset. Another quality control (QC) procedure was implemented after image processing (see Section 2.4 below).

2.3. Image processing

The CIVET 2.1.1 pipeline developed at the Montreal Neurological Institute was used to extract cortical surfaces on T1w images for corticometric analyses (<http://www.bic.mni.mcgill.ca/ServicesSoftware/CIVET-2-1-0-References>). In order to take into consideration brain volume variations between subjects, the native MR images were linearly registered to standardized MNI-Talairach space, based on the MNI-ICBM152 non-linear symmetric model (Collins et al., 1994; Fonov et al., 2009; Grabner et al., 2006; Mazziotta et al., 1995; Talairach and Tournoux, 1988). Intensity inhomogeneity introduced by the scanner was normalized via N3 (Sled et al., 1998). The images were then classified into cerebrospinal fluid, gray matter, white matter, and background image by a neural net classifier (INSECT) (Tohka et al., 2004; Zijdenbos et al., 2002). Cortical surfaces were derived with a marching-cubes algorithm (Lorensen et al.), ultimately demarcating 81,924 vertices on every subject's brain. Vertex correspondence is done via a Laplacian map method described in Kim et al. (2005). In the subjects' native space, new gray and white matter sampling surfaces were generated using the CIVET/2.1.1 function `average_surfaces`, which creates a surface whose vertex coordinates are the average of the vertex coordinates of the two input surfaces. The surface at 25% of the distance from the gray/white boundary to the pial boundary ('25% surface') was generated by first averaging the gray/white boundary and pial surfaces to create a surface that is 50% of the cortical distance, and then averaging the gray/white surface with the 50% surface. New white matter surfaces were generated at the same distance from the gray/white boundary surface as the gray matter surfaces, but in the direction of the white matter. Specifically, each new white matter surface was generated by first creating vectors between each vertex on the gray/white boundary surface and the corresponding vertex on the gray matter surfaces (separately for each gray matter surface generated). The vectors were then inverted in the x , y , and z dimensions and added to the coordinates of the gray/white boundary surface vertices, such that white matter surfaces were created at the same distance from the gray/white boundary as the gray matter surfaces, but in the opposite direction (toward the superficial white matter instead of toward the pial surface). To establish correspondence of these vertices between subjects, the cortical surfaces were registered non-linearly to a high-resolution average surface template of the ICBM152 data set (Boucher et al., 2009; Lyttelton et al., 2007; Robbins et al., 2004).

2.4. Quality control of processed images

The sensitivity of automated cortical measurements to scan-specific field distortions and to small movement artifacts has already been established (Reuter et al., 2015), and the need for a quality control of pipeline outputs is now considered necessary as failing to do so can significantly alter findings when it comes to developmental trajectories (Ducharme et al., 2016; Olafson et al., 2020).

As a first step, we applied the automated CIVET QC protocol which produces, for each subject, multiple quantitative metrics including number of self-intersecting and gray-white surface intersections, brain mask extraction errors, and percentage of error in expansion of

gray matter, among others: <http://www.bic.mni.mcgill.ca/ServicesSoftware/CIVET-1-1-12-Quality-Control>. After excluding problematic outputs, we then applied the same quality control procedure used by Ducharme et al. (2016). Two investigators (ACT and SK), blinded to all clinical variables, implemented quality control of the pipeline outputs by means of unanimous consent, according to previously established quality control criteria; note that SK was a co-investigator in the Ducharme et al. manuscript (2016). Specifically, processed scans were removed if they featured gross deformities, cropped areas in surfaces, and/or poor delineation between gray and white matter surfaces in large areas; for an example comparison between failed scans and an accepted one, see Supplementary Fig. 1.

In the process of QC, 113 scans were removed. From the remaining scans, some had missing information at visits, such as scanner identification or age, which amounted to another 90 scans to be removed. Additionally, prior to analysis, individual scans were removed if whole-brain mean contrast was more than three standard deviations from the mean of the sample - this led to removing only two scans, each from a different subject. A total of 819 scans from 394 participants were retained. There were 394 subjects with one timepoint, 290 subjects with two timepoints, and 135 subjects with three timepoints. Supplementary Fig. 2 shows the age distribution of our dataset. Under the NIHPD terminology, 296 participants were scanned at Visit 1, 313 participants were scanned at Visit 2, and 210 participants were scanned at Visit 3.

2.5. Gray-White contrast

GWC is defined here as the ratio of the intensities of white and gray matter on T1w MRI images after N3 correction. In the subjects' native space, we created a gray surface at 25% of the distance from the gray/white boundary to the pial boundary and a white surface at the same distance but in the direction of white matter. A relative distance to compute GWC was chosen in favor of a fixed distance due to the presence of extremely thin sections of cortex, wherein a fixed distance could, in some instances, lead to sampling at a distance greater than the thickness of the cortex. A relative sampling distance was also preferred over a fixed one to maximize chances of sampling from the vicinity of the same cortical layer(s) across the cortical mantle. The value of 25% was based on results from Whitaker et al. (2016), showing that the highest myelin concentration observable in the cortex is within the 20% to 30% range of local cortical thickness. To produce the final contrast measures, the sub-white surface values were divided by the gray surface values at each vertex; thus, a larger GWC value represents a sharper gray-white boundary. An example depicting the placement of the surfaces used to compute contrast at each vertex is found in Fig. 1. Finally, spatial surface blurring was applied using a Gaussian blur with FWHM of 20 mm.

2.6. Assessment of partial volume effects

Given that a voxel may be composed of a mixture of tissue types, an effect known as partial volume effect (PVE), and that such issues may have corollary consequences on our estimations of contrast, we examined PVE on our data. To do so, we used the trimmed minimum covariance determinant (TMCD) method as described by Tohka et al. (2004) for the estimation of the commonly used mixel PVE model (Choi et al., 1991). TMCD provides accurate and robust estimation of partial volume parameters that can be used for the correct

delineation of cortical surfaces (Tohka et al., 2004). Both the gray and white surfaces were examined for PVEs from surrounding tissue.

2.7. Statistical analyses

Whole-brain, vertex-wise analyses were conducted using Surfstat (<https://www.math.mcgill.ca/keith/surfstat/>), a statistical toolbox implemented in MATLAB. Mixed-effects model (with intercept as the random effect for each subject) were fit using residualized maximum likelihood estimation (REML). These mixed-effects regression models, which control for within-subject variance, can deal with multiple measures per subject, missing data, as well as irregular intervals between visits. By adding a random intercept in the model, we implicitly assume that observations within subjects are correlated, with a fixed correlation for each pair of observations. This model also allows to model subject-specific age trajectories, with a constant slope (for linear, quadratic, and cubic age effects) across subjects and subject-specific intercepts. Note that we don't have enough data points over time to include a random slope (and therefore a subject-specific slope) for the age coefficient. Non vertex-wise analyses were performed in R version 3.6.2 using the *nlme* package (Pinheiro et al., 2013). Results were thresholded using a 5% false discovery rate (FDR).

The following three models were applied across 77,122 vertices (brainstem and non-cortical midline are masked out) and the Akaike Information Criterion (AIC) was used to select the best fitting model for each vertex (Cavanaugh and Neath, 2019).

$$\begin{aligned} \text{Local GWC} = & \text{Intercept} + \text{Age}\beta_1 + \text{Age}^2\beta_2 + \text{Age}^3\beta_3 + \text{Sex}\beta_4 \\ & + \text{Scanner}\beta_5 + \text{random}(\text{subject}) + \text{Error} \end{aligned}$$

$$\begin{aligned} \text{Local GWC} = & \text{Intercept} + \text{Age}\beta_1 + \text{Age}^2\beta_2 + \text{Sex}\beta_3 \\ & + \text{Scanner}\beta_4 + \text{random}(\text{subject}) + \text{Error} \end{aligned}$$

$$\begin{aligned} \text{Local GWC} = & \text{Intercept} + \text{Age}\beta_1 + \text{Sex}\beta_2 \\ & + \text{Scanner}\beta_3 + \text{random}(\text{subject}) + \text{Error} \end{aligned}$$

The inclusion of the age variable allows for the implicit assessment of rate of change with time. The potential for interactions between age and sex was examined using SurfStat. Mixed-effects modeling was performed as described above, except with the inclusion of the appropriate Sex:Age interaction terms, again, based on the lowest AIC. Sex* Age, Sex* Age², and Sex* Age³ interactions were examined within full models including lower order interaction(s) for Sex* Age² and Sex* Age³. To showcase GWC trajectories in a variety of regions across the brain, mean GWC was calculated within a 3 mm radius circle along the surface (mean included vertices = 15) within each selected region. A radius of 3 mm was chosen in order to sample from a large enough area while avoiding sampling from different trajectory types (i.e. avoid examining a region where the center of the 3mm-radius circle is

within a region with a quadratic trajectory type while the perimeter is within a region with a linear trajectory type). To communicate regionality, the Desikan surface atlas labels were used (Desikan et al., 2006; Klein and Tourville, 2012). Mixed-effects models were fit as described above, with mean GWC as the dependent variable; the model type was determined by the prevailing model in the selected region, from the aforementioned whole-brain, vertex-wise analysis. To produce the scatterplots of each locale's progression, mean GWC was predicted from the model fits; modeling was performed independently for male- and female-only subsets of the data, in addition to the global curve derived from the full sample.

Finally, to visualize the dynamics of how maturation of GWC progresses across the brain, vertex-wise estimations of GWC trajectory were derived and mapped onto the cortical surface. Specifically, mixed-effects models were fit at each vertex, again based on lowest AIC from the original vertex-wise analysis. Two methods were used to help visualize, through time, the progression of GWC; in the first, the predicted GWC values were mean centered, and in the other, they were standardized via vertex-wise scaling between 0 and 1 using the R function `scales::rescale`. These modified vertex-wise GWC predictions were then color-coded and mapped onto the brain surface. A slight 3 mm smoothing was used to improve visualization. Five snapshots were chosen to depict progression throughout childhood and into late adolescence.

3. Results

3.1. Demographics

No statistically significant differences were found between the original sample and our quality-controlled subsamples in terms of gender distribution, ethnic representation and socioeconomic status (see Table 1 and Supplementary Tables 1 and 2). However, our Visit 1 subsample had a slightly higher mean age than the original NIH Visit 1 sample ($t = 3.17$, $p = 0.002$). This is because younger children had slightly higher QC failures likely due to having a more difficult time remaining still in the scanner (Reuter et al., 2015).

3.2. Results of the examination of partial volume effects

With a few exceptions, there was little evidence for significant PVE impacts on our results. This is seen in Supplementary Fig. 3, where average PVE estimates from surrounding tissue are mapped onto the gray and white surfaces that were used to estimate GWC. Not finding strong evidence for PVEs is compatible with the fact that the lowest mean thickness across the cortex, for the sample of scans in this work, was above 1.5 mm (i.e., above the 1 mm isotropic voxel size used in the vast majority of scanners in NIH Study of Normal Brain Development study). For the gray surface, essentially no cerebrospinal fluid PVE was detected. However, a few regions exhibited some white matter PVE effects. These included the dorsal pericentral areas as well as the medial and posterior lateral occipital regions, bilaterally. This was to be expected because these regions are known to exhibit deep myelin penetration (Carey et al., 2018). As for the white surface, some PVE was detected in the insular region, bilaterally.

3.3. Overview of gwc findings

As seen in Fig. 2, GWC undergoes widespread developmental change. Vertex-wise, mixed-effects modeling produced a map wherein approximately 99% of vertices attained significance under linear, quadratic, or cubic trajectories of development. Approximately 16% of vertices reflected linear developmental trajectories of GWC as likeliest, 20% depicted quadratic trajectories as likeliest, while 63% of vertices reflected cubic trajectories as likeliest. Overall, most trajectories evidenced trends of declining GWC with age. Models that showed trajectories of increasing GWC were sparse, with slopes close to zero, and were exclusively located in the temporal poles and the medial orbitofrontal cortex. The quadratic developmental trajectories all appeared to be concave downward. Trajectories were also remarkably symmetric between hemispheres, with a few exceptions, outlined below.

3.4. GWC findings on whole sample

Whole-brain mean GWC was found to follow a cubic developmental trajectory based upon the lowest AIC (see Fig. 3); this trajectory was shown to follow a downward/decreasing trend with time. Our vertex-wise estimates parallel this finding with the main GWC trajectory being cubic. The distribution of the likeliest trajectories (i.e. linear, quadratic or cubic) were highly symmetrical and showed negative associations between GWC and age across the majority of the brain (See Fig. 2 and Supplementary Fig. 4).

Modeling the estimated, region-specific developmental progression of GWC in a handful of representative regions (Figs. 4a and 4b) yielded several findings. Qualitative assessments of trajectories within regions depicting quadratic and cubic trajectories of development showed many areas where GWC declined at an increasing rate between the ages of 10 and 15 years and continued its decline well into late adolescence. The temporal, frontal and parietal lobes all mostly exhibited cubic trajectories of decreasing GWC, while the occipital lobe evidenced a mixture of linear and cubic downward trajectories. In the limbic regions, developmental trajectories were mixed between cubic and some linear trends. An example of this is the cingulate, with the anterior cingulate reflecting a linear trajectory, while the posterior cingulate was found to follow a cubic trend. The primary motor cortex also included some linear declining trajectories. Notably, the cuneus exhibited a mix of linear and cubic decline. The superior parietal lobule, posterior temporal lobe, and all the precuneus, bilaterally followed linear trajectories of decline. There were also two symmetrical, anterior-posterior strips on the superior frontal gyri, which were found to deviate from the predominant cubic trajectory in the surrounding region of the frontal lobe; the strip in the left superior frontal gyrus evidenced a linear maturational trajectory, while the strip in the right superior frontal gyrus was observed as having a quadratic trajectory.

While the majority of the brain was found to follow a trajectory of decline in GWC, a few noteworthy exceptions are reported as follows. The right lateral occipital lobe depicts increasing GWC, as does the left posterior cingulate. Additionally, there appears to be a slight delay in progression of GWC to its minimum in the orbitofrontal cortex, relative to that of the frontal cortex as a whole. Overall, the frontal cortex was estimated to reach its minimum GWC later (within our age range), when compared to the rest of the brain (See Supplementary Figures 5 and 6).

3.5. Sex differences

Vertex-wise analyses that examined the effect of sex on GWC yielded a few significant regions where females tended to have lower contrast values than males across the age range examined here. Regions with a significant sex contrast (males-females) included the cuneus and parts of the precuneus, the anterior cingulate, and a large section of the medial orbitofrontal cortex. Fig. 5 shows a selection of plots produced from the significant regions on the left hemisphere (see Supplementary Figure 7 for areas of significant sex effects on both hemispheres); estimated trajectories show females consistently exhibiting a lower GWC. No interaction between age and sex was found to be statistically significant.

4. Discussion

This work constitutes the first longitudinal study of GWC neurotypical development in a representative American population during the critical developmental period between childhood and early adulthood (Waber et al., 2007). The vertex-wise analysis of the changes in GWC during the development of children and adolescents in our sample yielded a mixture of linear, quadratic, or cubic trajectories as significant across nearly the whole cortical surface. The cubic trajectory was the one that was most frequently observed. Overall, these results predominantly showed globally declining GWC with age. We also observed that the whole-brain average GWC followed a declining cubic trajectory. This extends prior findings from Vidal-Piñero et al. (2016), who found GWC to decline from early adulthood to old age. Our findings also fit well with prior work from (Norbom et al., 2019), who found GWC to globally decrease with age in a cross-sectional analysis of a sample of subjects that included various types of psychopathology. When viewing the vertex-wise, regional, and average whole-brain GWC trajectories, the complexity of maturational changes in GWC throughout early-life development is apparent. A prominent finding was the remarkable symmetry across much of the cortical surface, regarding the best fitting model as seen in Fig. 2 and Supplementary Figure 4.

GWC in the frontal cortex appeared to show a delayed maturation as it manifested a decrease in contrast later than in the other regions, possibly reflecting the prolonged penetration of intracortical myelin (relative to the rest of the cortex) known to take place well past our examined age-range in this region (Bartzokis, 2004; Grydeland et al., 2019; Westlye et al., 2010). Speculation may suggest that healthy maturation of certain regions requires maintaining sharp boundaries between gray and white matter (i.e., high GWC) well into adulthood and old age. This view is compatible with results from Vidal-Piñero et al. (2016), who showed a positive association between symptoms of aging and lower GWC in the frontal cortex. Alternatively, Vidal-Piñero et al.'s (2016) results could simply reflect a higher starting point of GWC in early life (followed by a decrease in adulthood) for those having greater cognitive reserve.

In the cingulate cortex, our results quite elegantly show an obvious demarcation between the anterior and posterior cingulate, which fits well with the known cytoarchitectural and functional (e.g. error detection and emotional processing, respectively) roles of these two cingulate regions (Lane et al., 1998; Leech and Sharp, 2014; Leech and Smallwood, 2019; Stevens et al., 2011). A similar finding is visible on the insula (See Supplementary Figure 4),

where the inflated cortical surface clearly shows a demarcation that fits well with the known histological demarcation between the anterior agranular insula and the more posterior granular insula (Afif et al., 2010; Naqvi et al., 2014).

Our analyses evaluated the effect of sex on GWC, as well as whether there was a significant interaction between age and sex on GWC. Sex was found to have a significant effect (at 5% FDR) on GWC in several brain regions, across all three types of age trajectories. As shown in Fig. 5, males presented with slightly higher GWC than females in regions where a significant main effect of sex was found. No significant interaction effect on GWC was found anywhere across the cortical mantle for Age* Sex, Age²*Sex or Age³*Sex interactions. In keeping with this, male and female trajectories showed strikingly similar trajectories even though the plots were produced independently for the male and female samples.

The main effect of sex that is observed could potentially be linked to previously reported differences between males and females in both gray and white matter as informed by prior works. For instance, a study from Raznahan and colleagues found a higher percentage of gray matter tissue and interhemispheric connectivity in females, and higher percentage of white matter tissue and intrahemispheric connectivity in males (Raznahan et al., 2011). Ingahalikar et al. (2014) put forth strong evidence of differences in structural connectivity between males and females, with their results indicating that male brains are structured to facilitate intrahemispheric connectivity when compared to females, while female brains conversely had higher interhemispheric connectivity and cross-modular connections that would facilitate interhemispheric connectivity. Considering this, we propose that the widespread effect of sex on GWC reflects sex differences in intra-cortical patterns of myelination that support sex differences in connectivity profiles. In other words, we speculate that short- (intrahemispheric) and long- (interhemispheric) range connectivity is reflected by myelination patterns that lead to high and low GWC, respectively.

While the overall trend is of decreasing GWC, parts of the right lateral occipital lobe, temporal poles, parahippocampal gyrus, and orbitofrontal cortex were exceptions and exhibited trajectories of increasing or essentially level GWC. Given potentially altered MRI signal due to magnetic susceptibility between air-filled sinuses in the vicinity of some of these brain regions (Juchem et al., 2010) and/or to possible partial volume effects, both of which may have been too subtle to detect by QC in some cases, we consider the isolated findings of increasing GWC in some of these regions to potentially be artefactual (Du et al., 2007; Kharabian Masouleh et al., 2020; Reuter et al., 2015; Savalia et al., 2017). Regarding partial volume effects, it is noteworthy that such effects were shown to be present in the insula, uncus, parahippocampal gyrus (as mentioned above), dorsal pericentral, medial occipital, and posterior lateral occipital regions and making estimates of GWC in these regions as tentative.

It is important to keep in mind that the biological underpinnings of GWC and of variations in GWC are not yet clearly elucidated (Lewis et al., 2018; Raznahan et al., 2011; Salat et al., 2009). As our dataset lacks true data representing myelinated axons at the cortical boundary, we are bound to speculate on underpinnings of the negative trajectories of GWC change

observed here, while acknowledging the partial contribution from other sources that would affect GWC makeup, such as cellular iron content (Fukunaga et al., 2010). One possibility is that GWC changes reflect the selective pruning of gray matter in such a way that it would affect the ratio value of gray to white matter intensity (Elston et al., 2009). Another, perhaps more plausible alternative that is gaining traction is that contrast changes rather reflect the gradual invasion of the lower layers of cortex by myelin (Elston et al., 2009; Kharitonova et al., 2013; Petanjek et al., 2011; Rakic, 2002). If this is the case, our data may very well reflect genuine myelination of gray-matter fibers in the lower layers of the cortex. This assertion is supported by closer examinations of early life development around our given age-range (Deoni et al., 2015; Gilmore et al., 2012; Sowell et al., 2003). Indeed, various neuroimaging studies that used volumetric methods to measure growth of gray and white matter have shown a gradual decrease in gray matter volume that coincides with an increase in white matter volume (Courchesne et al., 2000; Giedd et al., 1999; Jernigan et al., 1991; Sowell et al., 2003; Sowell et al., 2004; Sowell et al., 2001). This is further supported by postmortem studies that show myelin penetration well into adolescence and a lack of significant loss of cortical neuronal cell bodies until the fourth or fifth decade of life (Dekaban and Sadowsky, 1978; Raznahan et al., 2011; Terry et al., 1987; Wang and Young, 2014), as well as by histological data that shows the cortical boundary as anything but discretely “black or white” (Annese et al., 2004). In fact, what is currently referred to as “cortical thinning” *in early life* may largely be attributed to myelination of neuronal fibers in the lower layers of the cortex, as opposed to physically smaller or fewer gray-matter neurons and associated processes (Sowell et al., 2004). In sum, myelination of intracortical gray matter fibers is likely responsible for most of the apparent reduction in GWC found in our data.

Having said this, we must also acknowledge that GWC could be calculated differently. For example, while our measure of GWC was based on a relative distance from the gray/white matter boundary (e.g., 25% distance from gray-white surface boundary to the pial surface), a fixed distance (e.g., 1 mm) or another relative distance could have been chosen instead. Alternatively, a relative distance within the gray-matter, and a fixed distance (e.g., 1 mm) into the white matter could have been possible as well. As discussed in the methods, for the gray surface, we favored a sampling distance that was relative to gray-matter thickness (instead of a fixed distance) to decrease the possibility of sampling from regions outside the cortex in areas of very thin cortex.

A caveat of the current work is that our age range may have influenced our observations. We propose, for instance, that quadratic or cubic trajectories of decline would emerge as likeliest in most regions where only a linear trend was observed, because the slope of a linear decrease is likely to attenuate at some point with age to avoid reaching a GWC of zero early in adulthood. This reasoning can also be extended to regions of quadratic trajectories that might follow a cubic trajectory had a larger age range been available in our cohort. Another caveat pertains to partial volume effects.

Ultimately, additional, and more expansive investigations will be required for elucidating the nature of GWC changes across the lifespan. For instance, future work on GWC would benefit from using scans with sub-millimeter voxel sizes readily achievable with higher field

strength (e.g., 3T). Such work would decrease potential partial volume effects, improve surface extraction, and could help improve our understanding of how GWC combines with other cortical metrics (e.g., cortical thickness). Also, further refinements in how GWC is calculated and using GWC to adjust estimates of other cortical metrics might help improve our characterization of brain development.

In summary, we find that the distribution of the best fitting GWC trajectory model is highly symmetrical across hemispheres and that the GWC tends to decrease with age during development over most of the brain. While the underlying neurobiology of GWC is not entirely clear, the current work, which constitutes the first longitudinal GWC study of the critical developmental period between childhood and early adulthood, adds to the growing body of knowledge on cortical development (Bartzokis, 2004; Deoni et al., 2015; Glasser et al., 2014; Glasser and Van Essen, 2011).

Supplementary Material

Refer to Web version on PubMed Central for supplementary material.

Acknowledgments

This project has been funded in whole or in part with Federal funds from the National Institute of Child Health and Human Development, the National Institute on Drug Abuse, the National Institute of Mental Health, and the National Institute of Neurological Disorders and Stroke (Contract #s N01-HD02-3343, N01-MH9-0002, and N01-NS-9-2314, -2315, -2316, -2317, -2319 and -2320). Special thanks to the NIH contracting officers for their support. SK is supported by a CIHR Young Investigator Salary Award. MA is supported by the NIMH (1K08MH121654) as well as a Young investigator Grant from the Brain & Behavior Foundation. We acknowledge the help of Claude Lepage and Vladimir Fonov for their valuable comments.

References

- Afif A, Minotti L, Kahane P, Hoffmann D, 2010. Anatomofunctional organization of the insular cortex: a study using intracerebral electrical stimulation in epileptic patients. *Epilepsia* 51 (11), 2305–2315. doi:10.1111/j.1528-1167.2010.02755.x. [PubMed: 20946128]
- Alexander-Bloch AF, Reiss PT, Rapoport J, McAdams H, Giedd JN, Bullmore ET, Gogtay N, 2014. Abnormal cortical growth in schizophrenia targets normative modules of synchronized development. *Biol. Psychiatry* 76 (6), 438–446. doi:10.1016/j.biopsych.2014.02.010. [PubMed: 24690112]
- Ameis SH, Ducharme S, Albaugh MD, Hudziak JJ, Botteron KN, Lepage C, ..., Karama S, 2014. Cortical thickness, cortico-amygdalar networks, and externalizing behaviors in healthy children. *Biol. Psychiatry* 75 (1), 65–72. doi:10.1016/j.biopsych.2013.06.008. [PubMed: 23890738]
- Annese J, Pitiot A, Dinov ID, Toga AW, 2004. A myelo-architectonic method for the structural classification of cortical areas. *Neuroimage* 21 (1), 15–26. doi:10.1016/j.neuroimage.2003.08.024. [PubMed: 14741638]
- Bartzokis G, 2004. Age-related myelin breakdown: a developmental model of cognitive decline and Alzheimer's disease. *Neurobiol. Aging* 25 (1), 5–18. doi:10.1016/j.neurobiolaging.2003.03.001. [PubMed: 14675724]
- Bezgin G, Lewis JD, Evans AC, 2018. Developmental changes of cortical white–gray contrast as predictors of autism diagnosis and severity. *Transl. Psychiatry* 8 (1), 249. doi:10.1038/s41398-018-0296-2, 249. [PubMed: 30446637]
- Boucher M, Whitesides S, Evans A, 2009. Depth potential function for folding pattern representation, registration and analysis. *Med. Image Anal* 13 (2), 203–214. doi:10.1016/j.media.2008.09.001. [PubMed: 18996043]

- Brain Development Cooperative, G., 2012. Total and regional brain volumes in a population-based normative sample from 4 to 18 years: the NIH MRI study of normal brain development. *Cerebr. Cortex* 22 (1), 1–12. doi:10.1093/cercor/bhr018.
- Carey D, Caprini F, Allen M, Lutti A, Weiskopf N, Rees G, ..., Dick F, 2018. Quantitative MRI provides markers of intra-, inter-regional, and age-related differences in young adult cortical microstructure. *Neuroimage* 182, 429–440. doi:10.1016/j.neuroimage.2017.11.066. [PubMed: 29203455]
- Cavanaugh JE, Neath AA, 2019. The Akaike information criterion: background, derivation, properties, application, interpretation, and refinements. *WIREs Comput. Stat* 11 (3), e1460. doi:10.1002/wics.1460.
- Choi HS, Haynor DR, Kim Y, 1991. Partial volume tissue classification of multichannel magnetic resonance images—a mixel model. *IEEE Trans. Med. Imaging* 10 (3), 395–407. doi:10.1109/42.97590. [PubMed: 18222842]
- Collins DL, Neelin P, Peters TM, Evans AC, 1994. Automatic 3D intersubject registration of MR volumetric data in standardized Talairach space. *J. Comput. Assist. Tomogr* 18 (2), 192–205. Retrieved from <http://www.ncbi.nlm.nih.gov/pubmed/8126267>. [PubMed: 8126267]
- Courchesne E, Chisum HJ, Townsend J, Cowles A, Covington J, Egaas B, ..., Press GA, 2000. Normal brain development and aging: quantitative analysis at in vivo MR imaging in healthy volunteers. *Radiology* 216 (3), 672–682. doi:10.1148/radiology.216.3.r00au37672. [PubMed: 10966694]
- Croteau-Chonka EC, Dean DC 3rd, Remer J, Dirks H, O’Muircheartaigh J, Deoni SCL 2016. Examining the relationships between cortical maturation and white matter myelination throughout early childhood. *Neuroimage* 125, 413–421. doi:10.1016/j.neuroimage.2015.10.038. [PubMed: 26499814]
- Dale AM, Fischl B, Sereno MI, 1999. Cortical surface-based analysis: I. Segmentation and surface reconstruction. *Neuroimage* 9 (2), 179–194. doi:10.1006/nimg.1998.0395. [PubMed: 9931268]
- Dekaban AS, Sadowsky D, 1978. Changes in brain weights during the span of human life: relation of brain weights to body heights and body weights. *Ann. Neurol* 4 (4), 345–356. doi:10.1002/ana.410040410. [PubMed: 727739]
- Deoni SCL, Dean DC 3rd, Remer J, Dirks H, O’Muircheartaigh J, 2015. Cortical maturation and myelination in healthy toddlers and young children. *Neuroimage* 115, 147–161. doi:10.1016/j.neuroimage.2015.04.058. [PubMed: 25944614]
- Desikan RS, Ségonne F, Fischl B, Quinn BT, Dickerson BC, Blacker D, ..., Killiany RJ, 2006. An automated labeling system for subdividing the human cerebral cortex on MRI scans into gyral based regions of interest. *Neuroimage* 31 (3), 968–980. doi:10.1016/j.neuroimage.2006.01.021. [PubMed: 16530430]
- Dosenbach NUF, Nardos B, Cohen AL, Fair DA, Power JD, Church JA, ..., Schlaggar BL, 2010. Prediction of individual brain maturity using fMRI. *Science* 329 (5997), 1358–1361. doi:10.1126/science.1194144. [PubMed: 20829489]
- Du YP, Dalwani M, Wylie K, Claus E, Tregellas JR, 2007. Reducing susceptibility artifacts in fMRI using volume-selective z-shim compensation. *Magn. Reson. Med* 57 (2), 396–404. doi:10.1002/mrm.21150. [PubMed: 17260355]
- Ducharme S, Albaugh MD, Hudziak JJ, Botteron KN, Nguyen TV, Truong C, ..., O’Neill J, 2014. Anxious/depressed symptoms are linked to right ventromedial prefrontal cortical thickness maturation in healthy children and young adults. *Cerebr. Cortex* 24 (11), 2941–2950. doi:10.1093/cercor/bht151.
- Ducharme S, Albaugh MD, Nguyen T-V, Hudziak JJ, Mateos-Pérez JM, Labbe A, ..., Brain Development Cooperative, G., 2016. Trajectories of cortical thickness maturation in normal brain development—the importance of quality control procedures. *Neuroimage* 125, 267–279. doi:10.1016/j.neuroimage.2015.10.010. [PubMed: 26463175]
- Ducharme S, Albaugh MD, Nguyen T-V, Hudziak JJ, Mateos-Pérez JM, Labbe A, ..., Brain Development Cooperative Group, f.t.B.D.C., 2015. Trajectories of cortical surface area and cortical volume maturation in normal brain development. *Data Brief* 5, 929–938. doi:10.1016/j.dib.2015.10.044. [PubMed: 26702424]

- Ducharme S, Hudziak JJ, Botteron KN, Albaugh MD, Nguyen T-V, Karama S, ..., Brain Development Cooperative Group, f.t.B.D.C., 2012. Decreased regional cortical thickness and thinning rate are associated with inattention symptoms in healthy children. *J. Am. Acad. Child Adolesc. Psychiatry* 51 (1), 18–27. doi:10.1016/j.jaac.2011.09.022, e12. [PubMed: 22176936]
- Elston GN, Oga T, Fujita I, 2009. Spinogenesis and pruning scales across functional hierarchies. *J. Neurosci* 29 (10), 3271–3275. doi:10.1523/JNEUROSCI.5216-08.2009. [PubMed: 19279264]
- Evans AC, Brain Development Cooperative, G., 2006. The NIH MRI study of normal brain development. *Neuroimage* 30 (1), 184–202. doi:10.1016/j.neuroimage.2005.09.068. [PubMed: 16376577]
- Fischl B, Sereno MI, Tootell RB, Dale AM, 1999. High-resolution intersubject averaging and a coordinate system for the cortical surface. *Hum. Brain Mapp* 8 (4), 272–284. Retrieved from <http://www.ncbi.nlm.nih.gov/pubmed/10619420>. [PubMed: 10619420]
- Fjell AM, Grydeland H, Krogstad SK, Amlie I, Rohani DA, Ferschmann L, ..., Walhovd KB, 2015. Development and aging of cortical thickness correspond to genetic organization patterns. *Proc. Natl. Acad. Sci. USA* 112 (50), 15462–15467. doi:10.1073/pnas.1508831112. [PubMed: 26575625]
- Fonov VS, Evans AC, McKinstry RC, Almlie CR, Collins DL, 2009. Unbiased non-linear average age-appropriate brain templates from birth to adulthood. *Neuroimage* 47, S102. doi:10.1016/S1053-8119(09)70884-5, -S102.
- Fukunaga M, Li T-Q, van Gelderen P, de Zwart JA, Shmueli K, Yao B, ..., Duyn JH, 2010. Layer-specific variation of iron content in cerebral cortex as a source of MRI contrast. *Proc. Natl. Acad. Sci. U.S.A* 107 (8), 3834–3839. doi:10.1073/pnas.0911177107. [PubMed: 20133720]
- Ghosh SS, Kakunoori S, Augustinack J, Nieto-Castanon A, Kovelman I, Gaab N, ..., Fischl B, 2010. Evaluating the validity of volume-based and surface-based brain image registration for developmental cognitive neuroscience studies in children 4 to 11 years of age. *Neuroimage* 53 (1), 85–93. doi:10.1016/j.neuroimage.2010.05.075. [PubMed: 20621657]
- Giedd JN, Blumenthal J, Jeffries NO, Castellanos FX, Liu H, Zijdenbos A, ..., Rapoport JL, 1999. Brain development during childhood and adolescence: a longitudinal MRI study. *Nat. Neurosci* 2 (10), 861–863. doi:10.1038/13158. [PubMed: 10491603]
- Giedd JN, Lalonde FM, Celano MJ, White SL, Wallace GL, Lee NR, Lenroot RK, 2009. Anatomical brain magnetic resonance imaging of typically developing children and adolescents. *J. Am. Acad. Child Adolesc. Psychiatry* 48 (5), 465–470. doi:10.1097/CHI.0b013e31819f2715. [PubMed: 19395901]
- Giedd JN, Rapoport JL, 2010. Structural MRI of pediatric brain development: what have we learned and where are we going? *Neuron* 67 (5), 728–734. doi:10.1016/j.neuron.2010.08.040. [PubMed: 20826305]
- Gilmore JH, Shi F, Woolson SL, Knickmeyer RC, Short SJ, Lin W, ..., Shen D, 2012. Longitudinal development of cortical and subcortical gray matter from birth to 2 years. *Cereb. Cortex* 22 (11), 2478–2485. doi:10.1093/cercor/bhr327. [PubMed: 22109543]
- Glasser MF, Goyal MS, Preuss TM, Raichle ME, Van Essen DC, 2014. Trends and properties of human cerebral cortex: correlations with cortical myelin content. *Neuroimage* 93, 165–175. doi:10.1016/j.neuroimage.2013.03.060. [PubMed: 23567887]
- Glasser MF, Van Essen DC, 2011. Mapping human cortical areas in vivo based on myelin content as revealed by T1- and T2-weighted MRI. *J. Neurosci* 31 (32), 11597–11616. doi:10.1523/JNEUROSCI.2180-11.2011. [PubMed: 21832190]
- Gogtay N, Giedd JN, Lusk L, Hayashi KM, Greenstein D, Vaituzis AC, ..., Thompson PM, 2004. Dynamic mapping of human cortical development during childhood through early adulthood. *Proc. Natl. Acad. Sci* 101 (21), 8174–8179. doi:10.1073/pnas.0402680101. [PubMed: 15148381]
- Grabner G, Janke AL, Budge MM, Smith D, Pruessner J, Collins DL, 2006. Symmetric atlas and model based segmentation: an application to the hippocampus in older adults. In: *Medical Image Computing and Computer-Assisted Intervention : MIC-CAI ... International Conference on Medical Image Computing and Computer-Assisted Intervention*, pp. 58–66 9(Pt 2) Retrieved from.

- Grydeland H, Vértes PE, Váša F, Romero-Garcia R, Whitaker K, Alexander-Bloch AF, ..., Bullmore ET, 2019. Waves of maturation and senescence in microstructural MRI markers of human cortical myelination over the lifespan. *Cerebr. Cortex* 29 (3), 1369–1381. doi:10.1093/cercor/bhy330.
- Grydeland H, Walhovd KB, Tamnes CK, Westlye LT, Fjell AM, 2013. Intracortical myelin links with performance variability across the human lifespan: results from T1- and T2-weighted MRI myelin mapping and diffusion tensor imaging. *J. Neurosci* 33 (47), 18618–18630. doi:10.1523/JNEUROSCI.2811-13.2013. [PubMed: 24259583]
- Ingalhalikar M, Smith A, Parker D, Satterthwaite TD, Elliott MA, Ruparel K, ..., Verma R, 2014. Sex differences in the structural connectome of the human brain. *Proc. Natl. Acad. Sci* 111 (2), 823. doi:10.1073/pnas.1316909110. [PubMed: 24297904]
- Jernigan TL, Traunker DA, Hesselink JR, Tallal PA, 1991. Maturation of human cerebrum observed in vivo during adolescence. *Brain* 114 (5), 2037–2049. doi:10.1093/brain/114.5.2037. [PubMed: 1933232]
- Juchem C, Nixon TW, McIntyre S, Rothman DL, de Graaf RA, 2010. Magnetic field homogenization of the human prefrontal cortex with a set of localized electrical coils. *Magn. Reson. Med* 63 (1), 171–180. doi:10.1002/mrm.22164. [PubMed: 19918909]
- Kabani N, Le Goualher G, MacDonald D, Evans AC, 2001. Measurement of cortical thickness using an automated 3-D algorithm: a validation study. *Neuroimage* 13 (2), 375–380. doi:10.1006/nimg.2000.0652. [PubMed: 11162277]
- Kharabian Masouleh S, Eickhoff SB, Zeighami Y, Lewis LB, Dahnke R, Gaser C, ..., Valk SL, 2020. Influence of processing pipeline on cortical thickness measurement. *Cerebr. Cortex* 30 (9), 5014–5027. doi:10.1093/cercor/bhaa097.
- Kharitonova M, Martin RE, Gabrieli JDE, Sheridan MA, 2013. Cortical gray-matter thinning is associated with age-related improvements on executive function tasks. *Dev. Cogn. Neurosci* 6, 61–71. doi:10.1016/j.dcn.2013.07.002. [PubMed: 23896579]
- Khundrakpam BS, Lewis JD, Zhao L, Chouinard-Decorte F, Evans AC, 2016. Brain connectivity in normally developing children and adolescents. *Neuroimage* 134, 192–203. doi:10.1016/j.neuroimage.2016.03.062. [PubMed: 27054487]
- Klein A, & Tourville J (2012). 101 labeled brain images and a consistent human cortical labeling protocol. In (Vol. 6, pp. 171–171).
- Lane RD, Reiman EM, Axelrod B, Yun L-S, Holmes A, Schwartz GE, 1998. Neural correlates of levels of emotional awareness: evidence of an interaction between emotion and attention in the anterior cingulate cortex. *J. Cogn. Neurosci* 10 (4), 525–535. doi:10.1162/089892998562924. [PubMed: 9712681]
- Lebel C, Beaulieu C, 2011. Longitudinal development of human brain wiring continues from childhood into adulthood. *J. Neurosci* 31 (30), 10937–10947. doi:10.1523/JNEUROSCI.5302-10.2011. [PubMed: 21795544]
- Leech R, Sharp DJ, 2014. The role of the posterior cingulate cortex in cognition and disease. *Brain* 137 (Pt 1), 12–32. doi:10.1093/brain/awt162. [PubMed: 23869106]
- Leech R, Smallwood J, 2019. Chapter 5 - The Posterior Cingulate Cortex: Insights from Structure and Function. Elsevier B. A. B. T. H. o. C. N. Vogt (Ed.), (Vol. 166, pp. 73–85).
- Lenroot RK, Gogtay N, Greenstein DK, Wells EM, Wallace GL, Clasen LS, ..., Giedd JN, 2007. Sexual dimorphism of brain developmental trajectories during childhood and adolescence. *Neuroimage* 36 (4), 1065–1073. doi:10.1016/j.neuroimage.2007.03.053. [PubMed: 17513132]
- Lerch JP, Evans AC, 2005. Cortical thickness analysis examined through power analysis and a population simulation. *Neuroimage* 24 (1), 163–173. doi:10.1016/j.neuroimage.2004.07.045. [PubMed: 15588607]
- Lewis JD, Evans AC, Tohka J, Brain Development Cooperative, G., Pediatric Imaging, N., Genetics, S., 2018. T1 white/gray contrast as a predictor of chronological age, and an index of cognitive performance. *Neuroimage* 173, 341–350. doi:10.1016/j.neuroimage.2018.02.050. [PubMed: 29501876]
- Lytelton O, Boucher M, Robbins S, Evans A, 2007. An unbiased iterative group registration template for cortical surface analysis. *Neuroimage* 34 (4), 1535–1544. doi:10.1016/j.neuroimage.2006.10.041. [PubMed: 17188895]

- Magnaldi S, Ukmar M, Vasciaveo A, Longo R, Pozzi-Mucelli RS, 1993. Contrast between white and grey matter: MRI appearance with ageing. *Eur. Radiol* 3 (6), 513–519. doi:10.1007/BF00169600.
- Mazziotta JC, Toga AW, Evans A, Fox P, Lancaster J, 1995. A probabilistic atlas of the human brain: theory and rationale for its development. The International Consortium for Brain Mapping (ICBM). *Neuroimage* 2 (2), 89–101. Retrieved from <http://www.ncbi.nlm.nih.gov/pubmed/9343592>. [PubMed: 9343592]
- Mills KL, Goddings A-L, Herting MM, Meuwese R, Blakemore S-J, Crone EA, ..., Tamnes CK, 2016. Structural brain development between childhood and adulthood: convergence across four longitudinal samples. *Neuroimage* 141, 273–281. doi:10.1016/j.neuroimage.2016.07.044. [PubMed: 27453157]
- Mills KL, Lalonde F, Clasen LS, Giedd JN, Blakemore S-J, 2014. Developmental changes in the structure of the social brain in late childhood and adolescence. *Soc. Cogn. Affect. Neurosci* 9 (1), 123–131. doi:10.1093/scan/nss113. [PubMed: 23051898]
- Muñoz-Moreno E, Fischi-Gomez E, Batalle D, Borradori-Tolsa C, Eixarch E, Thiran J-P, ..., Hüppi PS, 2016. Structural brain network reorganization and social cognition related to adverse perinatal condition from infancy to early adolescence. *Front. Neurosci* 10, 560. doi:10.3389/fnins.2016.00560, 560. [PubMed: 28008304]
- Naqvi NH, Gaznick N, Tranel D, Bechara A, 2014. The insula: a critical neural substrate for craving and drug seeking under conflict and risk. *Ann. N. Y. Acad. Sci* 1316, 53–70. doi:10.1111/nyas.12415. [PubMed: 24690001]
- Norbom LB, Doan NT, Alnæs D, Kaufmann T, Moberget T, Rokicki J, ..., Tamnes CK, 2019. Probing brain developmental patterns of myelination and associations with psychopathology in youths using gray/white matter contrast. *Biol. Psychiatry* 85 (5), 389–398. doi:10.1016/j.biopsych.2018.09.027. [PubMed: 30447910]
- Norbom LB, Rokicki J, Alnæs D, Kaufmann T, Doan NT, Andreassen OA, ..., Tamnes CK, 2020. Maturation of cortical microstructure and cognitive development in childhood and adolescence: a T1w/T2w ratio MRI study. *Hum. Brain Mapp* doi:10.1002/hbm.25149, n/a(n/a).
- Olafson E, Bedford S, Devenyi GA, Patel R, Tullo S, Park MTM, ..., Chakravarty MM, 2020. Examining the boundary sharpness coefficient as an index of cortical microstructure and its relationship with age and sex in autism spectrum disorder 2020.2007.2009.196212-192020.196207.196209.196212 doi:10.1101/2020.07.09.196212.
- Patel Y, Shin J, Drakesmith M, Evans J, Pausova Z, Paus T, 2020. Virtual histology of multi-modal magnetic resonance imaging of cerebral cortex in young men. *Neuroimage* 218, 116968. doi:10.1016/j.neuroimage.2020.116968, 116968. [PubMed: 32450248]
- Petanjek Z, Judaš M, Šimic G, Rasin MR, Uylings HBM, Rakic P, Kostovic I, 2011. Extraordinary neoteny of synaptic spines in the human prefrontal cortex. *Proc. Natl. Acad. Sci. USA* 108 (32), 13281–13286. doi:10.1073/pnas.1105108108. [PubMed: 21788513]
- Postelnicu G, Zollei L, Fischl B, 2009. Combined volumetric and surface registration. *IEEE Trans. Med. Imaging* 28 (4), 508–522. doi:10.1109/TMI.2008.2004426. [PubMed: 19273000]
- Rakic P, 2002. Neurogenesis in adult primate neocortex: an evaluation of the evidence. *Nat. Rev. Neurosci* 3 (1), 65–71. doi:10.1038/nrn700. [PubMed: 11823806]
- Raz N, Lindenberger U, Rodrigue KM, Kennedy KM, Head D, Williamson A, ... Acker JD, 2005. Regional brain changes in aging healthy adults: general trends, individual differences and modifiers. *Cerebr. Cortex* 15 (11), 1676–1689. doi:10.1093/cercor/bhi044.
- Raznahan A, Shaw P, Lalonde F, Stockman M, Wallace GL, Greenstein D, ... Giedd JN, 2011. How does your cortex grow? *J. Neurosci* 31 (19), 7174–7177. doi:10.1523/JNEUROSCI.0054-11.2011. [PubMed: 21562281]
- Reuter M, Tisdall MD, Qureshi A, Buckner RL, van der Kouwe AJW, Fischl B, 2015. Head motion during MRI acquisition reduces gray matter volume and thickness estimates. *Neuroimage* 107, 107–115. doi:10.1016/j.neuroimage.2014.12.006. [PubMed: 25498430]
- Robbins S, Evans AC, Collins DL, Whitesides S, 2004. Tuning and comparing spatial normalization methods. *Med. Image Anal* 8 (3), 311–323. doi:10.1016/j.media.2004.06.009. [PubMed: 15450225]

- Rowley CD, Bazin P-L, Tardif CL, Sehmbi M, Hashim E, Zaharieva N, ..., Bock NA, 2015. Assessing intracortical myelin in the living human brain using myelinated cortical thickness. *Front. Neurosci* 9, 396. 396 Retrieved from <https://www.frontiersin.org/article/10.3389/fnins.2015.00396>. [PubMed: 26557052]
- Salat DH, Lee SY, van der Kouwe AJ, Greve DN, Fischl B, Rosas HD, 2009. Age-associated alterations in cortical gray and white matter signal intensity and gray to white matter contrast. *Neuroimage* 48 (1), 21–28. doi:10.1016/j.neuroimage.2009.06.074. [PubMed: 19580876]
- Savalia NK, Agres PF, Chan MY, Feczko EJ, Kennedy KM, Wig GS, 2017. Motion-related artifacts in structural brain images revealed with independent estimates of in-scanner head motion. *Hum. Brain Mapp* 38 (1), 472–492. doi:10.1002/hbm.23397. [PubMed: 27634551]
- Shaw P, Eckstrand K, Sharp W, Blumenthal J, Lerch JP, Greenstein D, ... Rapoport JL, 2007. Attention-deficit/hyperactivity disorder is characterized by a delay in cortical maturation. *Proc. Natl. Acad. Sci. USA* 104 (49), 19649–19654. doi:10.1073/pnas.0707741104. [PubMed: 18024590]
- Shaw P, Gilliam M, Liverpool M, Weddle C, Malek M, Sharp W, ..., Giedd J, 2011. Cortical development in typically developing children with symptoms of hyperactivity and impulsivity: support for a dimensional view of attention deficit hyperactivity disorder. *Am. J. Psychiatry* 168 (2), 143–151. doi:10.1176/appi.ajp.2010.10030385. [PubMed: 21159727]
- Shaw P, Greenstein D, Lerch J, Clasen L, Lenroot R, Gogtay N, ..., Giedd J, 2006a. Intellectual ability and cortical development in children and adolescents. *Nature* 440 (7084), 676–679. doi:10.1038/nature04513. [PubMed: 16572172]
- Shaw P, Kabani NJ, Lerch JP, Eckstrand K, Lenroot R, Gogtay N, ..., Wise SP, 2008. Neurodevelopmental trajectories of the human cerebral cortex. *J. Neurosci* 28 (14), 3586–3594. doi:10.1523/JNEUROSCI.5309-07.2008. [PubMed: 18385317]
- Shaw P, Lerch J, Greenstein D, Sharp W, Clasen L, Evans A, ..., Rapoport J, 2006b. Longitudinal mapping of cortical thickness and clinical outcome in children and adolescents with attention-deficit/hyperactivity disorder. *Arch. Gen. Psychiatry* 63 (5), 540. doi:10.1001/archpsyc.63.5.540, 540. [PubMed: 16651511]
- Sled JG, Zijdenbos AP, Evans AC, 1998. A nonparametric method for automatic correction of intensity nonuniformity in MRI data. *IEEE Trans. Med. Imaging* 17 (1), 87–97. doi:10.1109/42.668698. [PubMed: 9617910]
- Sowell ER, Peterson BS, Thompson PM, Welcome SE, Henkenius AL, Toga AW, 2003. Mapping cortical change across the human life span. *Nat. Neurosci* 6 (3), 309–315. doi:10.1038/nn1008. [PubMed: 12548289]
- Sowell ER, Thompson PM, Leonard CM, Welcome SE, Kan E, Toga AW, 2004. Longitudinal mapping of cortical thickness and brain growth in normal children. *J. Neurosci* 24 (38), 8223–8231. doi:10.1523/JNEUROSCI.1798-04.2004. [PubMed: 15385605]
- Sowell ER, Thompson PM, Tessner KD, Toga AW, 2001. Mapping continued brain growth and gray matter density reduction in dorsal frontal cortex: inverse relationships during postadolescent brain maturation. *J. Neurosci* 21 (22), 8819–8829. doi:10.1523/JNEUROSCI.21-22-08819.2001. [PubMed: 11698594]
- Stevens FL, Hurley RA, Taber KH, Hurley RA, Hayman LA, Taber KH, 2011. Anterior cingulate cortex: unique role in cognition and emotion. *J. Neuropsychiatry Clin. Neurosci* 23 (2), 121–125. doi:10.1176/jnp.23.2.jnp121. [PubMed: 21677237]
- Talairach J, Tournoux P, 1988. *Co-planar Stereotaxic Atlas of the Human Brain : 3-Dimensional Proportional System : an Approach to Cerebral Imaging*. G. Thieme
- Tannes CK, Herting MM, Goddings A-L, Meuwese R, Blakemore S-J, Dahl RE, ..., Mills KL, 2017. Development of the cerebral cortex across adolescence: a multisample study of inter-related longitudinal changes in cortical volume, surface area, and thickness. *J. Neurosci* 37 (12), 3402–3412. doi:10.1523/JNEUROSCI.3302-16.2017. [PubMed: 28242797]
- Tannes CK, Walhovd KB, Dale AM, Østby Y, Grydeland H, Richardson G, ..., Alzheimer's Disease Neuroimaging, I., 2013. Brain development and aging: overlapping and unique patterns of change. *Neuroimage* 68, 63–74. doi:10.1016/j.neuroimage.2012.11.039. [PubMed: 23246860]

- Terry RD, DeTeresa R, Hansen LA, 1987. Neocortical cell counts in normal human adult aging. *Ann. Neurol* 21 (6), 530–539. doi:10.1002/ana.410210603. [PubMed: 3606042]
- Thompson PM, Andreassen OA, Arias-Vasquez A, Bearden CE, Boedhoe PS, Brouwer RM, ..., Ye J, 2017. ENIGMA and the individual: predicting factors that affect the brain in 35 countries worldwide. *Neuroimage* 145, 389–408. doi:10.1016/j.neuroimage.2015.11.057. [PubMed: 26658930]
- Thompson PM, Giedd JN, Woods RP, MacDonald D, Evans AC, Toga AW, 2000. Growth patterns in the developing brain detected by using continuum mechanical tensor maps. *Nature* 404 (6774), 190–193. doi:10.1038/35004593. [PubMed: 10724172]
- Thormodsen R, Rimol LM, Tamnes CK, Juuhl-Langseth M, Holmén A, Emblem KE, ..., Agartz I, 2013. Age-related cortical thickness differences in adolescents with early-onset schizophrenia compared with healthy adolescents. *Psychiatry Res.: Neuroimaging* 214 (3), 190–196. doi:10.1016/j.psychres.2013.07.003.
- Tohka J, Zijdenbos A, Evans A, 2004. Fast and robust parameter estimation for statistical partial volume models in brain MRI. *Neuroimage* 23 (1), 84–97. doi:10.1016/J.NEUROIMAGE.2004.05.007. [PubMed: 15325355]
- Vidal-Piñero D, Walhovd KB, Storsve AB, Grydeland H, Rohani DA, Fjell AM, 2016. Accelerated longitudinal gray/white matter contrast decline in aging in lightly myelinated cortical regions. *Hum. Brain Mapp* 37 (10), 3669–3684. doi:10.1002/hbm.23267. [PubMed: 27228371]
- Waber DP, De Moor C, Forbes PW, Amlı CR, Botteron KN, Leonard G, ..., Rumsey J, 2007. The NIH MRI study of normal brain development: performance of a population based sample of healthy children aged 6 to 18 years on a neuropsychological battery. *J. Int. Neuropsychol. Soc* 13 (5), 729–746. doi:10.1017/S1355617707070841. [PubMed: 17511896]
- Wang S, Young KM, 2014. White matter plasticity in adulthood. *Neuroscience* 276, 148–160. doi:10.1016/j.neuroscience.2013.10.018. [PubMed: 24161723]
- Westlye LT, Walhovd KB, Dale AM, Bjørnerud A, Due-Tønnessen P, Engvig A, ..., Fjell AM, 2010. Differentiating maturational and aging-related changes of the cerebral cortex by use of thickness and signal intensity. *Neuroimage* 52 (1), 172–185. doi:10.1016/j.neuroimage.2010.03.056. [PubMed: 20347997]
- Whitaker KJ, Vértes PE, Romero-Garcia R, Váša F, Moutoussis M, Prabhu G, ... Bullmore ET (2016). Adolescence is associated with genomically patterned consolidation of the hubs of the human brain connectome. *Proc. Natl. Acad. Sci. USA*, 113(32), 9105–9110. doi:10.1073/pnas.1601745113 [PubMed: 27457931]
- Zhou D, Lebel C, Treit S, Evans A, Beaulieu C, 2015. Accelerated longitudinal cortical thinning in adolescence. *Neuroimage* 104, 138–145. doi:10.1016/j.neuroimage.2014.10.005. [PubMed: 25312772]
- Zielinski BA, Prigge MBD, Nielsen JA, Froehlich AL, Abildskov TJ, Anderson JS, ..., Lainhart JE, 2014. Longitudinal changes in cortical thickness in autism and typical development. *Brain* 137 (Pt 6), 1799–1812. doi:10.1093/brain/awu083. [PubMed: 24755274]
- Zijdenbos AP, Forghani R, Evans AC, 2002. Automatic "pipeline" analysis of 3-D MRI data for clinical trials: application to multiple sclerosis. *IEEE Trans. Med. Imaging* 21 (10), 1280–1291. doi:10.1109/TMI.2002.806283. [PubMed: 12585710]

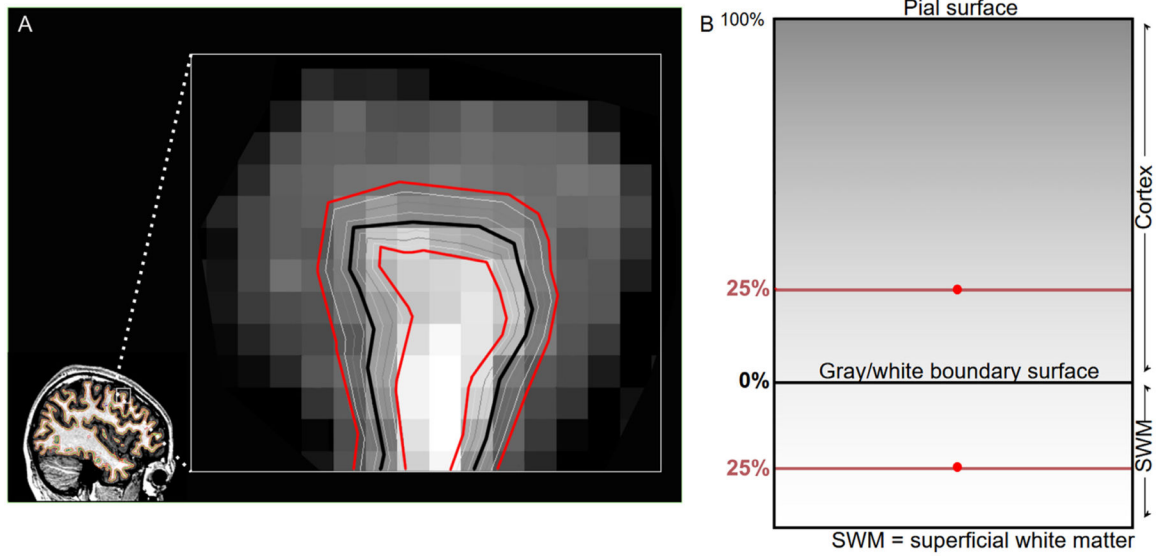


Fig. 1.
Calculation of GWC, Example showing the placement of the 25% distance surfaces in the gray matter and superficial white matter.

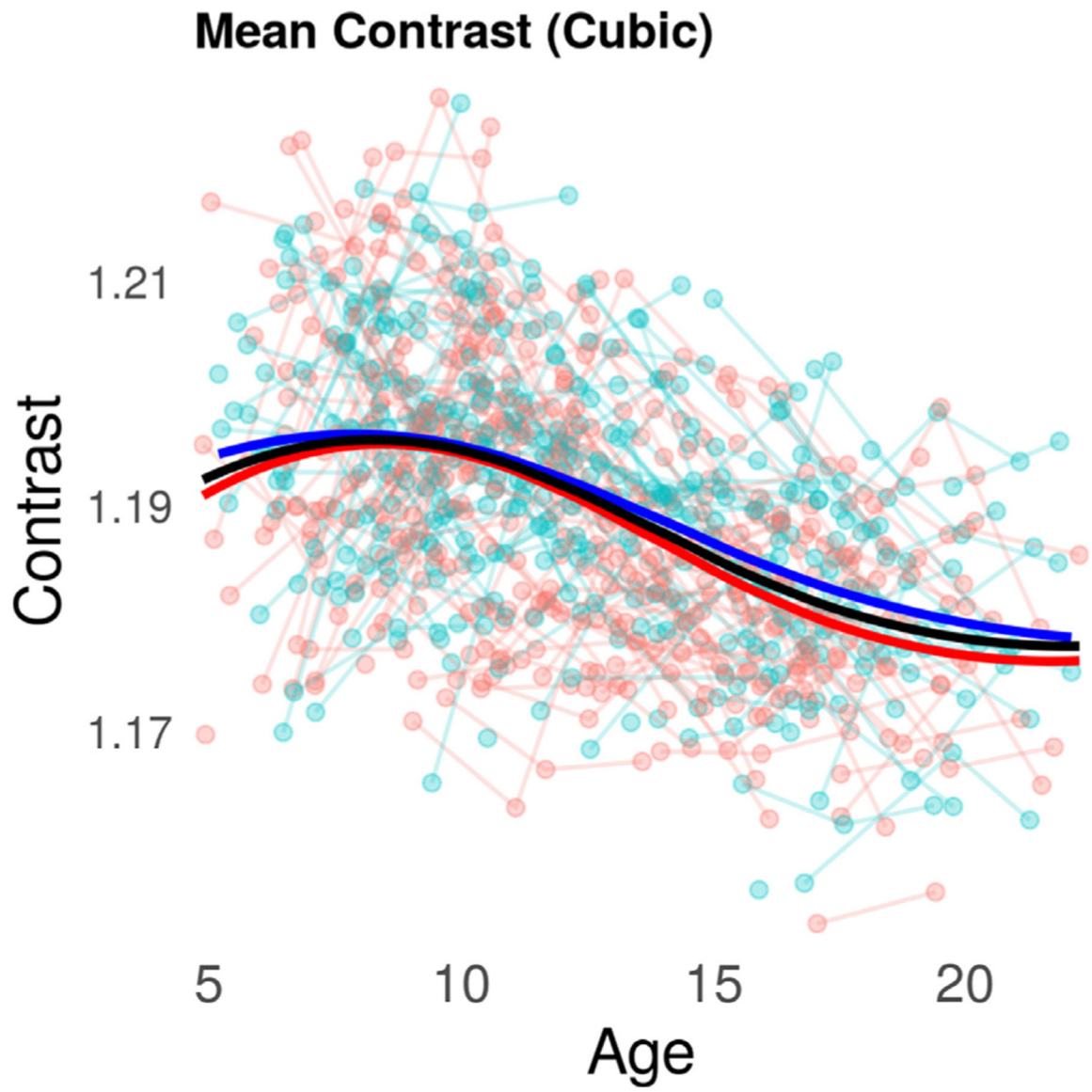
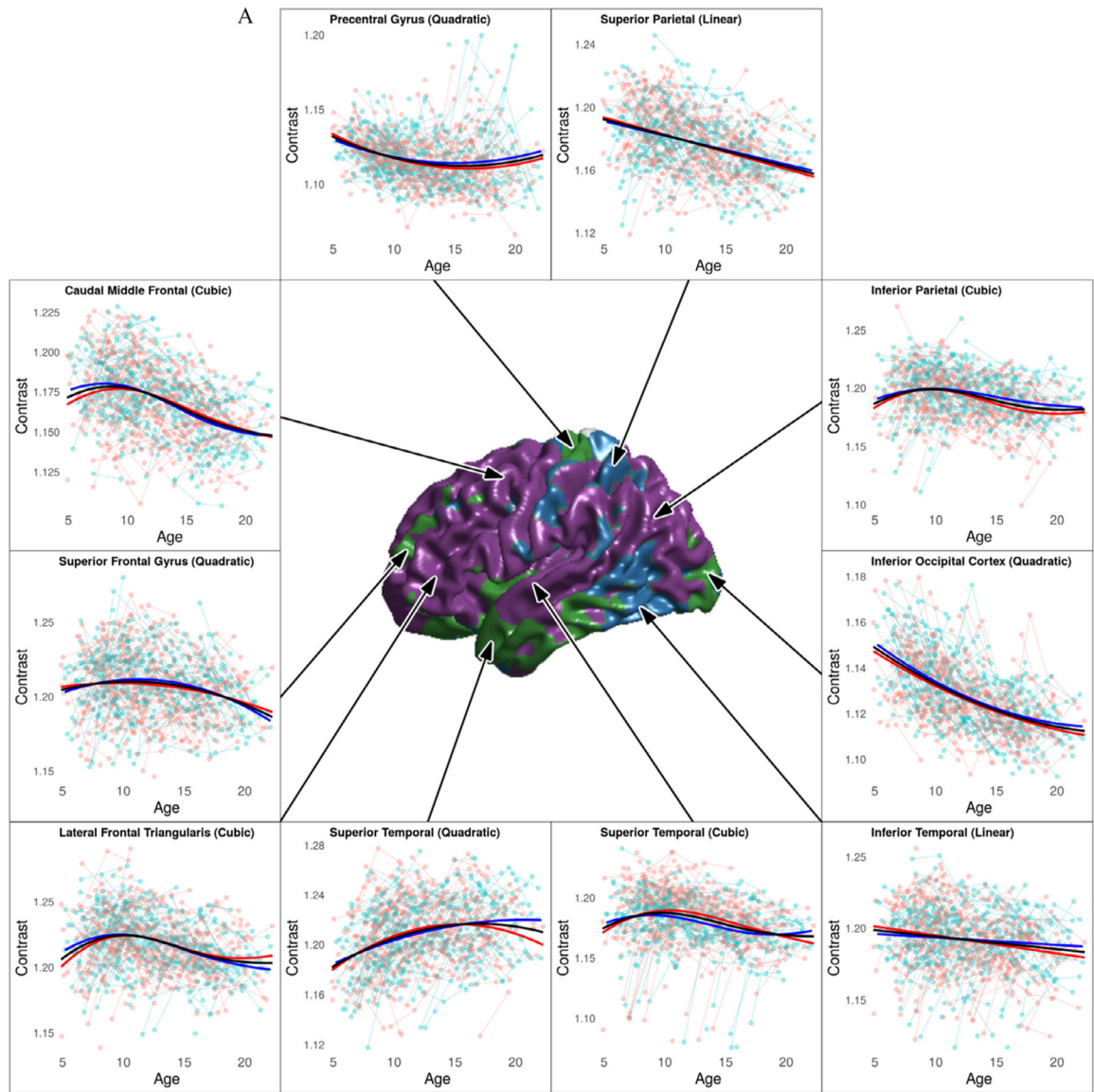


Fig. 3. Cubic age trajectory of whole-brain, mean GWC. Black curve is derived from the model prediction on the full sample. The blue and red curves represent predictions from modeling performed on the male- and female-only subsets of the data, respectively.



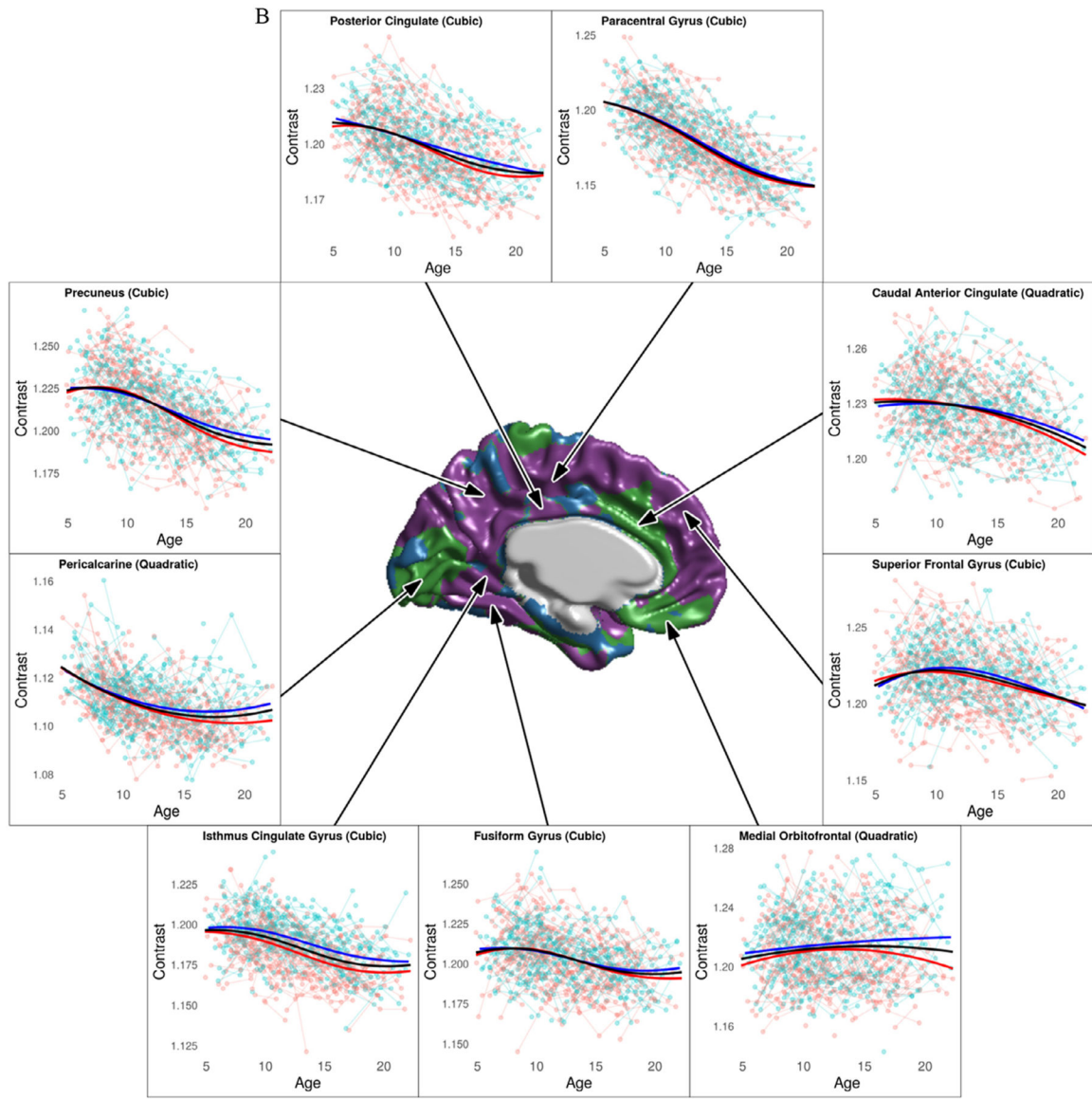


Fig. 4.

A. Qualitative overview of developmental trajectories of GWC, on the left lateral cortical surface. Black curves are derived from the model prediction on the full sample. The blue and red curves represent predictions from modeling performed on male- and female-only subsets of the data, respectively, and better reflect the true trajectories of males and females in our data. Even if these are not perfectly parallel to the global trajectory, there is no statistically significant ‘sex by age’ interaction. **B. Qualitative overview of developmental trajectories of GWC, on the left medial cortical surface.** Black curves are derived from the model prediction on the full sample. The blue and red curves represent predictions from modeling performed on male- and female-only subsets of the data, respectively, and better reflect the true trajectories of males and females in our data. Even if these are not perfectly parallel to the global trajectory, there is no statistically significant ‘sex by age’ interaction.

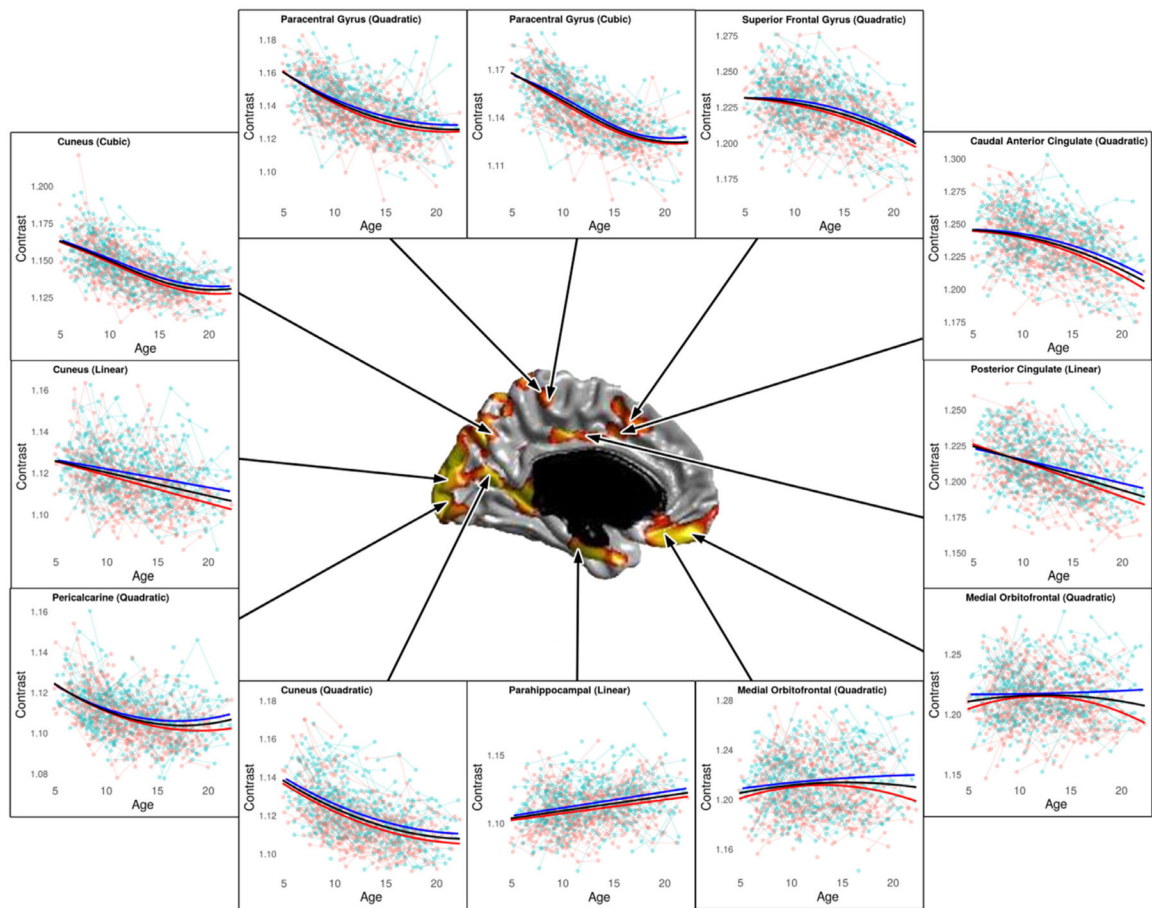


Fig. 5. Estimated trajectories of GWC maturation across various representative regions exhibiting a significant sex effect on GWC.

Black curves are derived from the model prediction on the full sample. The blue and red curves represent predictions from modeling performed on male- and female-only subsets of the data, respectively, and better reflect the true trajectories of males and females in our data. Even if these are not perfectly parallel to the global trajectory, there is no statistically significant ‘sex by age’ interaction.

Sample comparison between the original NIHPD Objective 1, Visit 1 sample, and the Visit 1 sample used in this study. When appropriate, means \pm standard deviations are provided.

Table 1

Sample	Objective 1 Visit 1 (<i>n</i> = 433)	Accepted Visit 1 Sample (<i>n</i> = 296)	Statistics (if applicable)
Age (Years)	10.4 \pm 3.8 (4.6 to 18.3 years)	11.3 \pm 3.7 (4.9 to 18.3 years)	<i>t</i> = 3.17, <i>p</i> < 0.002
Proportion of Males	48%	45.2%	χ^2 = 0.301, <i>p</i> = 0.583
Proportion of low/medium/high adjusted SES ^a	24.4% / 40.8% / 34.8%	22.6% / 41.2% / 36.1%	χ^2 = 0.185, <i>p</i> = 0.912
Proportion of Caucasians/African American/Other ^b	73.5% / 8.4% / 18.1%	74.7% / 8.4% / 16.9%	χ^2 = 0.099, <i>p</i> = 0.951

^aBased on the US Department of Housing and Urban Development method for comparing family income levels as a function of regional costs of living.

^bThe 'Other' category includes American Indian, Alaskan Native, Asian, Native Hawaiian or Other Pacific Islander, and those for whom ethnicity or race was not provided, or whose parents came from different racial or ethnic backgrounds.